Reconfigurable Antennas

Randy L. Haupt and Michael Lanagan

Haupt Associates
8493 Baseline Rd, Boulder, CO 80303 USA
Tel: +1 (303) 736-8132; E-mail: haupt@ieee.org

The Pennsylvania State University
263 Materials Research Laboratory, University Park, PA 16802 USA
Tel: +1 (814) 865-6992; Fax: +1 (814) 865-2326; E-mail: mxl46@psu.edu

Abstract

Reconfigurable antennas change polarization, operating frequency, or far-field pattern in order to cope with changing system parameters. This paper reviews some of the past and current technology applicable to reconfigurable antennas, with several examples of implementations. Mechanically movable parts and arrays are discussed, as well as more-recent semiconductor-component and tunable-material technologies applicable to reconfigurable antennas.

Keywords: Reconfigurable antennas; reconfigurable arrays; antenna arrays; wideband antennas; reflector antennas; microstrip patch antennas

1. Introduction

To configure means to arrange or organize the parts of something to achieve a purpose. For instance, configuring a microstrip antenna consists of determining the patch shape, substrate parameters, type and location of the feed, etc., in order for the antenna to radiate at a desired frequency and polarization. If the desired operating characteristics of the antenna change, then the antenna must be reconfigured or rebuilt to meet the new specifications. Reconfigurable antennas change their performance characteristics by altering the current flow on an antenna, using mechanically movable parts, phase shifters, attenuators, diodes, tunable materials, or active materials. A reconfigurable antenna can be a single antenna or an array.

A reconfigurable antenna modifies the antenna's pattern, polarization, or frequency/bandwidth in some desirable fashion. For instance, a reconfigurable antenna might steer or place a null in an antenna's pattern, switch from right-hand circularly polarized to left-hand circularly polarized, or move the resonant frequency from 2 GHz to 2.4 GHz. In this way, a single antenna replaces two or more antennas, in order to achieve multiple goals. Arrays are the ultimate reconfigurable antenna, because they have many avenues for controlling the current across the aperture. A reconfigurable array may have reconfigurable elements, or a reconfigurable array may change the amplitude and phase of each element, the number of active elements, the elements' positions, or the polarization.

The idea of reconfiguring an antenna is relatively old. In the early 1930s, the nulls of a two-element array were steered by using a calibrated variable phase changer in order to determine the direction of arrival of a signal [1]. Bruce and Beck changed the size of the rhombic antenna in Figure 1 by stretching the wires with a motor and weights [2]. The element lengths of the rhombus were 184 m, and the interior angles were between 132° and 164°. Reconfiguring the antenna consisted of adjusting the distance of the major axis by more than 100 m. Changing the shape of the rhombic wire antenna steered the beam in elevation. The Multiple-Unit Steerable Antenna (MUSA) was a six-element array of rhombic antennas with phase shifters at five of the elements [3]. A linear phase shift steered the main beam. This concept was perfected and introduced for azimuth scanning with a 14-row by three-column array of polyrod antennas. This array had 13 rotary phase changers for beam steering [4]. The Wullenweber array was invented during WW II. It is a large direction-finding circular array with a narrow beam that scans 360° in azimuth by activating a small group of adjacent elements along the circle [5].

In 1979, "reconfigurability" was defined as "the ability to adjust beam shapes upon command" [6]. The authors used

ISSN 1045-9243/2012/$26 ©2013 IEEE

a six-beam antenna to dynamically change the coverage area for a communications satellite. Several additional papers reported other reconfigurable space-based arrays. In the 1990s, a research group in England described their efforts to alter the reflecting surface of a parabolic-reflector antenna in order to control the radiation pattern [7]. From the mid-1990s until the present, reconfigurable-antenna projects have mostly involved microstrip antennas, and various semiconductor technologies applied to altering the current flow on the microstrip antenna. Bernhard wrote an excellent overview of reconfigurable antennas, with many examples [8].

This paper is an introduction/tutorial on reconfigurable-antenna technology. It begins with the oldest technology, mechanically movable parts and arrays, and then transitions to the more-recent semiconductor-component and tunable-material technologies. A detailed explanation of the technology with background information and examples are given. Some of the interesting material technologies, such as active materials, are promising for reconfigurable antennas with low loss at high frequencies.

2. Mechanically Movable Parts

The first reconfigurable antennas had mechanically movable parts (as in Figure 1). Large reflector antennas moved feeds to steer the main beam, or interchanged feed antennas to change frequency bands. An excellent example is the Arecibo spherical-reflector antenna, shown in Figure 2. A Gregorian dome and a carriage house with linear antennas are on either side of a curved track, called the azimuth arm. Electric motors move the Gregorian dome and carriage house many meters from vertical to 20° off vertical, in addition to rotating 360° in azimuth, in order to steer the main beam. Inside the Gregorian dome, the secondary and tertiary reflectors focus the radiation onto one of several receiving antennas, which can be moved into position using a large rotating platform. Hanging below the carriage house are various linear antennas, each tuned to a narrow band of frequencies. A second example is a beam-waveguide antenna. This type of Cassegrain reflector guides the signal by mirrors, from its normal focal point near the vertex, to a focal point below the structural support (Figure 3) [9]. The rotating reflector at the base of the antenna steers the signal to an appropriate feed. In this way, a single reflector antenna can cover a very broad frequency range.

It is also possible to place nulls in the antenna pattern by altering the reflector's surface. One approach to reconfiguring a reflector's surface is to move scattering plates near the surface to cause cancellation of interfering signals entering the sidelobes [10, 11]. Distorting a mesh-reflector's surface using electrostatic controls is another possible approach [7, 12]. The scattering from a small distorted part of the reflector is sufficient to place a null in a sidelobe.

3. Reconfigurable Arrays

Most reconfigurable arrays control the array pattern in order to steer the beam, place a null, modify the main beam shape, or change the sidelobe levels. There have been several applications that involve changing the polarization or frequency of operation, as well. The textbook approach to reconfiguring an array has adjustable amplitude and/or phase weights at each element. The literature on these arrays is vast, and will not be covered here. A digital beamformer significantly enhances the ability of the array to control the radiation pattern, since all the reconfiguring is done in software.

Beam control is possible by turning elements on and off in the array, as was mentioned earlier with a Wullenweber array.

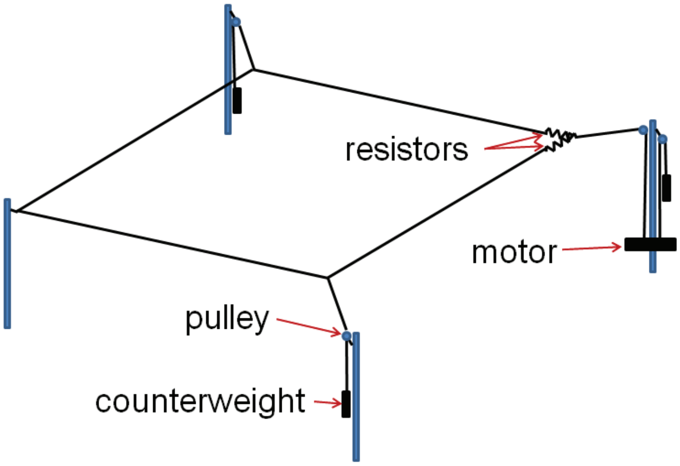

Figure 1. A steerable horizontal rhombic antenna.

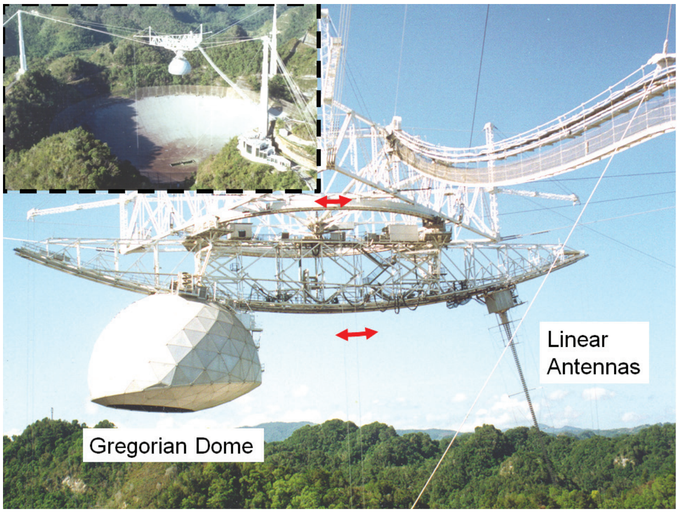

Figure 2. A blown-up picture of the feed for the Arecibo antenna (upper left) (photos courtesy of the NAIC – Arecibo Observatory, a facility of the NSF).

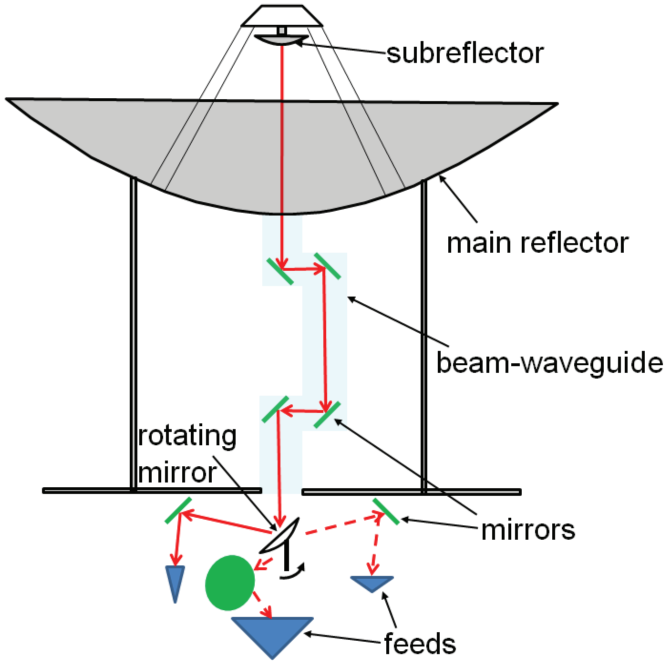

Figure 3. A diagram of a beam-waveguide antenna.

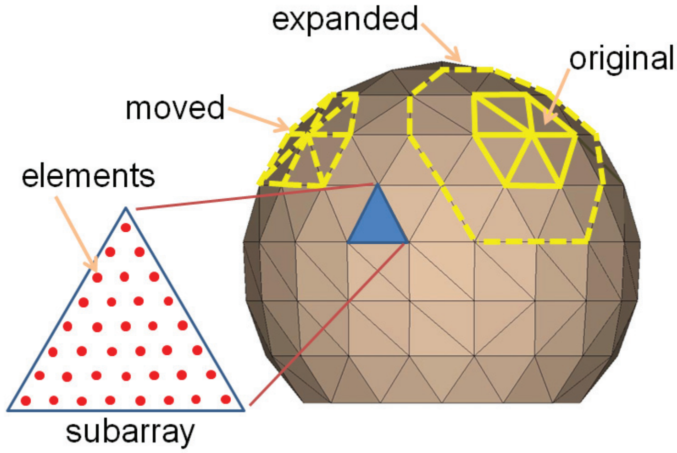

Figure 4. A phased array built on a geodesic dome. The yellow regions represent regions of activated subarrays.

Figure 4 shows this concept extended to a spherical array that was implemented on a geodesic dome. Each triangle on the dome was a subarray [13]. The active aperture was formed by combining the outputs from adjacent subarrays. Including more subarrays expanded the original active aperture (Figure 4). The active aperture could be moved to another location on the dome in order to point the main beam in a different direction. Other reconfigurable arrays that make use of switching an element on and off include dynamically thinning an array as one way to alter the sidelobe levels and nulls in order to reject interference [14], and time-modulated arrays that lower the average sidelobe levels by quickly switching elements on and off, with on times proportional to the desired amplitude of the element weight [15].

Another approach to reconfiguring an array is to physically move elements. Some very large reflector-antenna arrays use this concept. For instance, the Atacama Large Millimeter/sub-millimeter Array, or ALMA, will be a radio telescope composed of 66 12 m and 7 m parabolic dishes in Chile's Andes Mountains (Figure 5) [16]. The telescope will operate at frequencies from 31.25 GHz to 950 GHz. Array configurations from 250 m to 15 km will be possible. The ALMA antennas will be moved between flat concrete slabs by a special vehicle, as shown in Figure 5. A second example is the Very Large Array (VLA) radio telescope in New Mexico, built from 27 dish antennas that are 25 m in diameter [17]. Elements are placed in a Y shape, and can be changed by moving the elements along a railroad track (Figure 6). Four possible configurations, with aperture sizes of 36 km, 10 km, 3.6 km, or 1 km, are used. The array can operate between 73 MHz and 50 GHz.

The idea of moving elements to form a desired array aperture also extends to space. For instance, the TechSat 21 project investigated creating a large sparse antenna array by placing antenna elements on small spacecraft, and assembling the aperture with a formation of the satellites [18]. Beam formation was a function of the satellite constellation and the weighting of the signals.

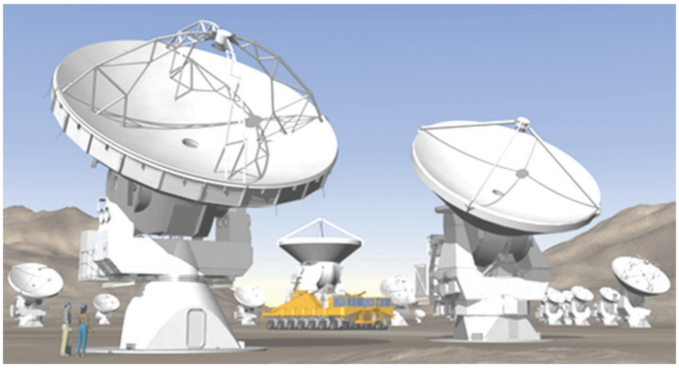

Figure 5. An artist's concept of ALMA (ESO/NAOJ/NRAO).

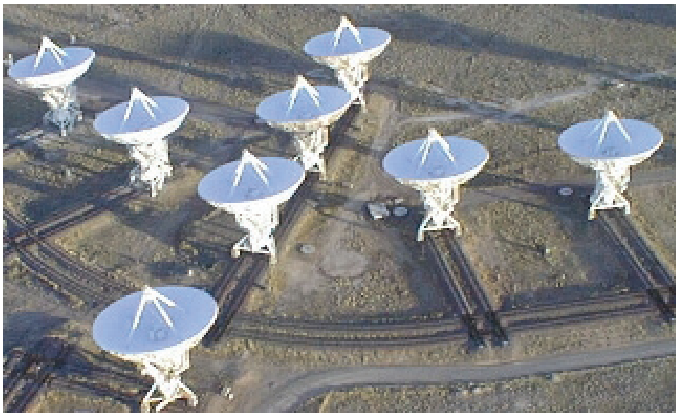

Figure 6. The VLA antennas on railroad tracks (NRAO/AUI/NSF).

4. RF Switches

An RF switch serves to open or close a current path on a reconfigurable antenna. A popular way to build a reconfigurable antenna is to connect various pieces of the antenna with RF switches. Opening and closing switches guides the current in a desirable path that changes the antenna's radiation properties, as well as its impedance.

RF switches may be mechanical or semiconductor. A switch is an open circuit when no actuation voltage is applied, and a low-impedance path for the RF signal when an actuation voltage is applied. The switch can be implemented in a series or shunt configuration. Some important characteristics of a switch are [19]:

- Characteristic impedance: if the switch is non-reflective, then it is matched to the transmission path; otherwise, it is reflective. The VSWR or return loss indicate the degree of matching.
- Bandwidth: some switches are low-pass filters (pass dc), while others are bandpass filters.
- Topology: is the switch normally on or off?
- Insertion loss and isolation: the ratio between the switch's output and input powers when the switch is on and off, respectively.
- Switching speed: the on time for a switch is defined by the time from when the control pulse reaches 50% of its level to the time that the RF signal is at 90% of its peak. The off time for a switch is defined by the time from when the control pulse reaches 50% of its level to the time that the RF signal is at 10% of its peak. Switching time is the larger of the on and off switch times.
- Expected life time: measured in number of switch actuations until failure.
- Power handling: measured in watts.

Below microwave frequencies, a low-pass switch acts like a resistor (R_{on}) when on, and a capacitor (C_{off}) when off. In contrast, a bandpass switch behaves like one capacitor when on, and a different capacitor when off. As the frequency increases, the ground inductance, bond-wire inductance, and transmission-line properties become significant factors, and complicate the circuit model. Parasitic resistances in the switch limit the upper-frequency bound. A switch figure-of-merit (FOM) is the cutoff frequency [20]:

$$f_c = \frac{1}{2\pi C_{off} R_{on}} . \tag{1}$$

A rule of thumb for the highest operating frequency for the switch is approximately $f_c/10$ [21].

The switching speeds of semiconductor switches are of the order of nanoseconds, while the switching speeds of mechanical switches are of the order of milliseconds. System constraints may limit the type of switch used, based on required switching times.

Switches can be used to reconfigure microstrip-patch antennas in several different ways. For instance, Figure 7 shows a two-dimensional array of metal patches on a substrate [22]. The sides of adjacent patches are connected with RF switches, in order to configure a desirable patch antenna. Figure 8 is an example of a patch with slots that can be shorted, in order to switch between polarizations [23].

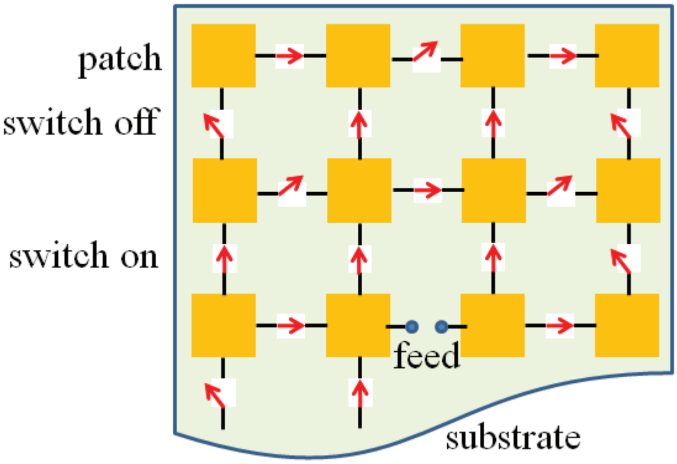

Figure 7. Reconfigurable microstrip patches.

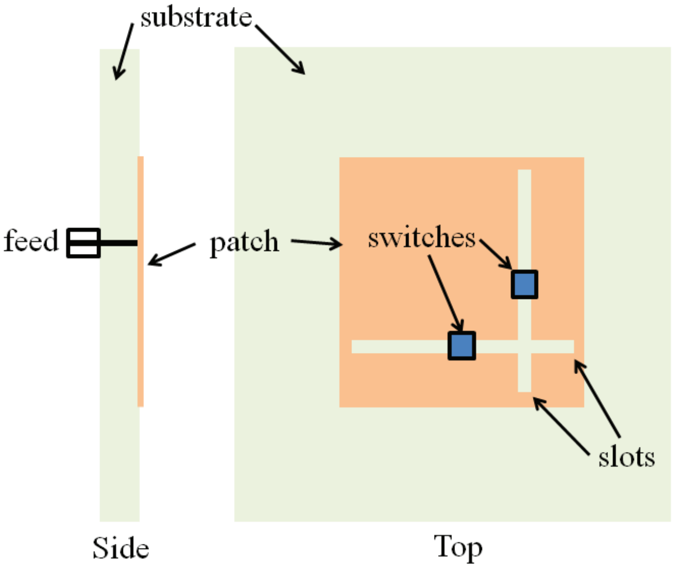

Figure 8. A reconfigurable slotted-patch antenna.

4.1 Semiconductor Switch

Figure 9 is a diagram of a field-effect transistor (FET) switch. Increasing the voltage at the gate increases the conducting channel's size beneath the gate, and allows current to flow between the source and drain. FET switches come in several varieties. Metal-semiconductor field-effect transistor (MESFET) and pseudomorphic high-electron-mobility transistor (PHEMT) switches are two variations, which are compared in Table 1. The authors in [24] suggested using FET switches in a configuration similar to Figure 7. The RF switch array was controlled with a light-emitting-diode backplane, which isolated the control circuitry from the RF paths in the antenna.

Another widely used microwave switch is the PIN diode [25]. It has heavily doped p-type and n-type regions (used for ohmic contacts), which are separated by a wide, lightly-doped intrinsic region (Figure 10). Forward biasing a PIN diode creates a very low resistance at high frequencies, while reverse biasing results in an open circuit. The PIN diode is current controlled, and can handle one or more amps of RF current. The authors in [23] suggested using PIN-diode switches for the configuration in Figure 8.

Table 1 compares the characteristics of FET and PIN-diode switches. Some notable differences between the two types of switches are [26, 27]:

- PIN diodes are current controlled, while FETs are voltage controlled. FETs require only a voltage signal for switching, instead of a dc current. This means that they have essentially zero dc power consumption, compared to the 10 mW or so it takes to turn on a PIN diode.

- PIN diodes have the ability to control large RF signal power while using much smaller levels of control power.

- PIN diodes are less susceptible to electrostatic-discharge (ESD) damage.

- The off-capacitance of PIN diodes is a function of reverse voltage: the more negative the voltage, the less capacitance.

- For FETs, the capacitance is not a strong function of reverse voltage.

- PIN diodes have a higher figure-of-merit than FETs. The useful upper-frequency-response limit of PIN diodes can be much higher, due to lower off-state capacitance (C_{off}) for a given on resistance (R_{on}).

Recently, a reconfigurable patch antenna was demonstrated in which the resonant frequency was altered between 2 GHz and 2.25 GHz, when the electrical length of a spiral-shaped slot in the patch was modified by a biased diode [28].

4.2 MEMS Switches

MEMS switches are tiny mechanical switches made on a substrate (silicon, quartz, glass) [29]. Unlike the PIN-diode and FET switches, a MEMS switch is mechanical. Figure 11 shows three types of MEMS switches in their on and off positions. The cantilever beam in Figures 11a and 11b is anchored to a post on the left, while the other end of the beam is suspended above the drain. An electrostatic force pulls the beam

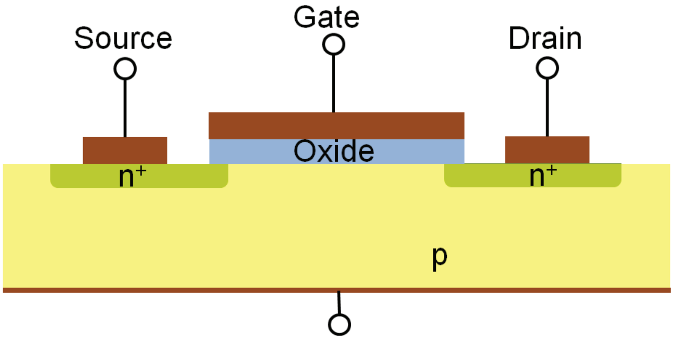

Figure 9. A diagram of a FET.

Table 1. A comparison of FET and PIN-diode switches [21].

	1 µm MESFET	0.25 µm PHEMT	Silicon PIN diode
Number of terminals	3	3	2
Typical on resistance	1.5 ohm-mm	1.2 ohm-mm	1.7 ohms
Typical off capacitance	0.40 pF/mm	0.32 pF/mm	0.05 pF
FOM (Eq. 1)	265 GHz	414 GHz	1872 GHz
Breakdown voltage	15 V	8 V	50 V
Lower frequency limit	dc	dc	10 MHz
Driver circuit complexity	low	low	high
Driver requirements	0 V on; –5 V off	+0.5 V on; –5 V off	5 to 10 mA on; 0 to –30 V off

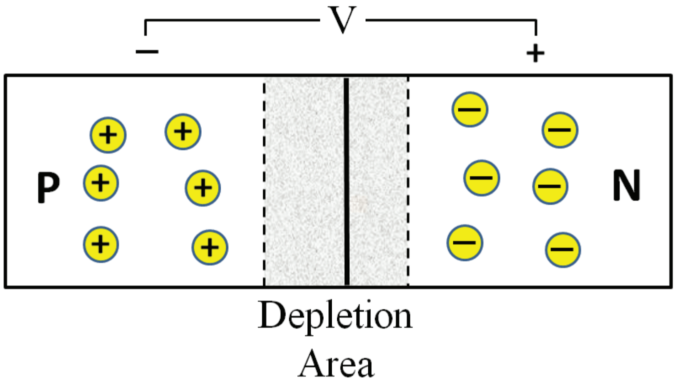

Figure 10. A diagram of a PIN diode.

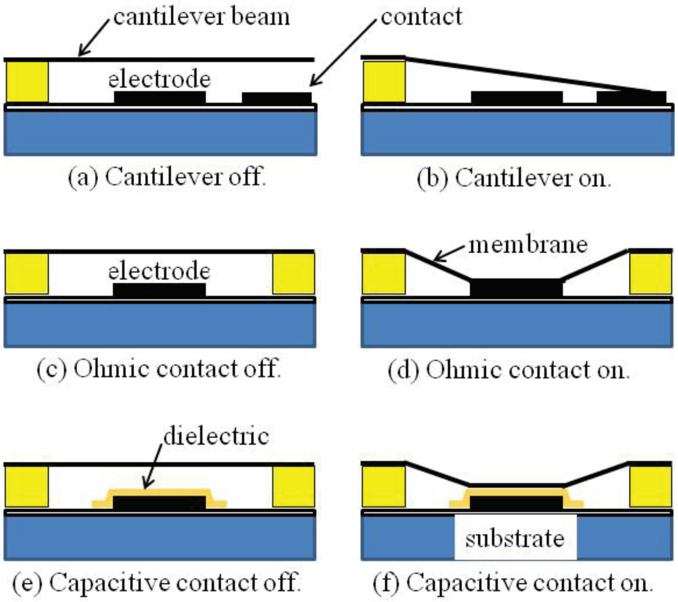

(a) Cantilever off. (b) Cantilever on.

(c) Ohmic contact off. (d) Ohmic contact on.

(e) Capacitive contact off. (f) Capacitive contact on.

Figure 11. Three types of MEMS switches in the on and off positions.

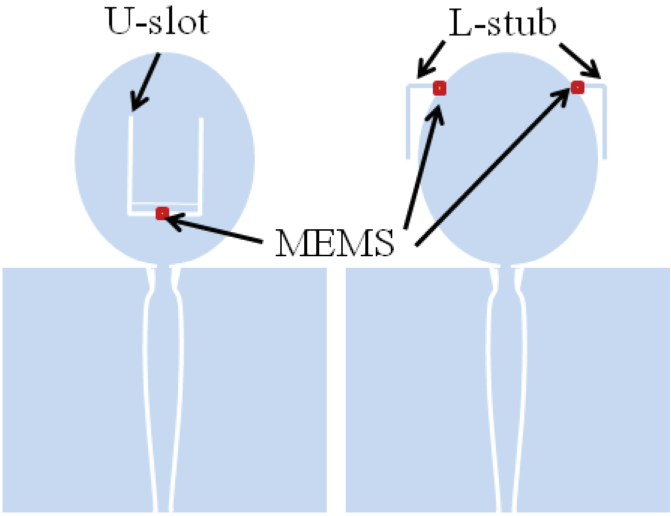

Figure 12. A diagram of the reconfigurable U-slot and L-stub antennas.

down when a voltage is applied, and creates an electrical path between the beam and the drain. Figures 11c-11f show a MEMS membrane switch, which consists of a flexible, thin, metal membrane, anchored to posts at both ends. A potential applied to the bias electrode pulls the membrane down and closes the circuit. An ohmic contact is a metal-to-metal connection, while a capacitive contact has a dielectric between the two metal contacts. Ohmic switches have a higher bandwidth than capacitive switches. The capacitive MEMS switches handle higher peak power levels and tolerate environmental effects better than ohmic contacts. The figure-of-merit for MEMS switches was reported at 9000 GHz [20]. Switching speeds for electro-statically driven capacitor structures are 10 µs. Recently, MEMS switches with piezoelectric films have been developed, and have fast switching times (1-2 µs). The cantilever device travels 6 µm between the on and off states [30].

MEMS switches have low power consumption, low insertion loss, and high isolation, like mechanical switches, but are small, light weight, and low cost, like semiconductor switches [31]. On the other hand, MEMS switches have high losses at microwave and mm-wave frequencies, limited power-handling capability (~100 mW), and they may need expensive packaging to protect the movable MEMS bridges against the environment.

MEMS switches have been proposed for use in reconfigurable antennas since the late 1990s [29]. For example, two ultra-wideband monopoles with a reconfigurable band notch in the wireless-LAN frequency range (5.150 GHz to 5.825 GHz) are shown in Figure 12 [32]. The antenna was an elliptical patch, fed with a coplanar-waveguide line. The U-shaped slot was approximately $\lambda/2$ long, and had a frequency notch when the MEMS switch was open, but not when the MEMS switch was closed. When the switch was open at 5.8 GHz, the currents in the inner and outer side of the slot flowed in opposite directions and cancelled each other. When the MEMS switch was closed, the slot was shorted at its center point, so the total length of the slot was cut in half. Consequently, the slot no longer supported the resonating currents, and radiation occurred as if the slot was not present.

The second antenna in Figure 12 had two inverted-L-shaped open stubs that connected and disconnected the stubs from the elliptical patch via MEMS switches. Shorting the stubs to the patch created a rejection band. At the resonance frequency, the direction of the current on the stub flowed in the opposite direction to the current along the nearby edge of the radiator, so the radiated fields cancelled. When the stubs were not shorted, the antenna operated over the whole UWB range (3.1 GHz to 10.6 GHz) without any rejection band. The MEMS switches actuated through the RF signal path, without any dc bias lines that might have complicated the switch's fabrication and integration, while degrading the radiation performance due to RF leakage through the bias.

Reconfigurable antennas can also change the antenna's polarization. For instance, placing MEMS switches in the feeds of microstrip antennas provides the ability to switch from one linear polarization to the orthogonal linear polarization, or to circular polarization, as shown in Figure 13 [33].

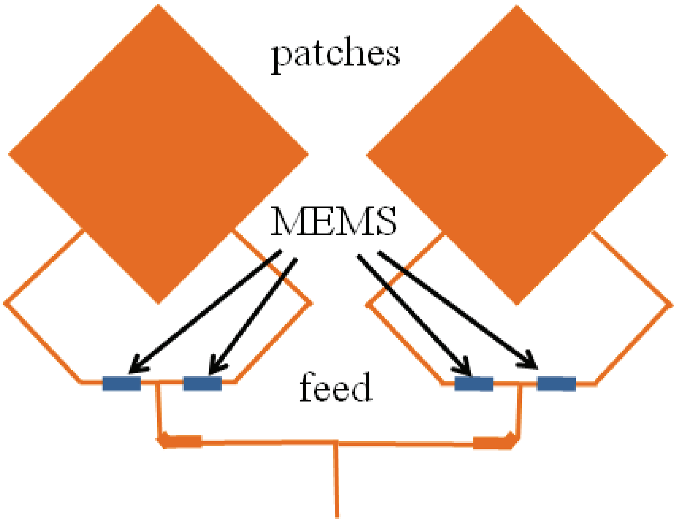

Figure 13. A reconfigurable antenna that changes polarization using MEMS.

MEMS structures are fabricated using a number of techniques, including etching trenches in the substrate, or building a multilayer structure on a planar substrate. Future research and development activities will need to address the cost and scalability of the MEMS process for large arrays. There are several important substrate properties that must be controlled, including surface roughness, permittivity, and dielectric loss. Recently, low-cost liquid-polymer substrates with $\varepsilon_r = 3$ and $\tan\delta = 0.002$ have been shown to be viable substrates for MEMS devices [34].

5. Varactors

Unlike the PIN diode, a varactor diode has a very thin depletion layer that acts like the insulating dielectric, and the P and N regions that act like the conducting plates (Figure 10). The capacitance is inversely proportional to the square root of the applied voltage, since the thickness of the depletion layer increases with the reverse bias. Varactors have a high-to-low capacitance ratio that is typically six over a voltage change of 0 V to 12 V.

Varactors are useful for tuning the antenna's frequency range. For instance, varactors were placed at the radiating edges of a microstrip-patch antenna in order to increase its very narrow bandwidth to a bandwidth of about 30% [35]. Strategically placing varactors along a slot antenna produced dual bands, with controllable first and second resonant frequencies [36]. A reconfigurable partially-reflecting-surface (PRS) antenna was built. It had a measured realized gain that varied from 10 dBi to 16.4 dBi over the tuning range of 5.2 GHz to 5.95 GHz, as the bias voltage was tuned from 6.49 V to 18.5 V [37]. The antenna had a partially-reflecting-surface material on the top surface, and a phase-agile surface below a microstrip patch. One phase-agile reflection cell was a microstrip-patch resonator, with varactor diodes that varied the resonant frequency of the patch antenna's reflection phase. The 13.5% tuning range extended the operating-frequency range by six times. The antenna's tuning bandwidth was limited by the varactor diode's tuning range for the phase-agile cells, and the antenna's efficiency was limited by the varactor diode's series resistance. A slotted-monopole antenna, modified with a varactor, could be tuned between 1.6 GHz and 2.3 GHz without a significant change in the antenna's efficiency [38]. Radiation pattern control has also been demonstrated using varactors [39].

6. Tunable Materials

Prospective devices with performance rivaling varactors will be based on materials that have tunable electrical, magnetic, and mechanical properties. For example, the propagation wavelength within the RF structure or impedance will be altered by permittivity (ε_r) or permeability (μ_r) changes, and the ability to tune the structure will be fundamentally related to the magnitudes of ε_r and μ_r [40]. Tunable mechanical strain alters either the effective length of the antenna, or modifies the impedance through capacitive coupling. Many concepts, such as tunable permeability, have been previously studied for microwave and millimeter-wave phase shifters [41]. Future tunable materials and devices will advance antenna technology through miniaturization and integration. A representative list of potential technologies for reconfigurable antennas is summarized in Table 2.

6.1 Tunable Conductivity

Conductivity in semiconductors can be tuned through changes in temperature, bias, or light. The conductivity of a semiconductor varies depending on the bandgap energy and the level of doping, and depending on defects in the material. Shining light with a photon energy greater than the bandgap on an intrinsic semiconductor increases the free-electron and hole-charge carriers, which in turn increases the semiconductor's conductivity. Solar cells are a good example.

Applying an electric field to a polymer electrolyte-silver-polyaniline composite alters the material from a state of low to high conductivity. Polymer composites with controllable resistance at microwave frequencies have stable, reproducible switching over more than 1000 test cycles [49].

Phase-change chalcogenides, such as $Ge_2Sb_2Te_5$ (proposed for non-volatile memory applications), also have tunable conductivity. Measurements have demonstrated that amorphous chalcogenides maintain low conductivity values into the GHz frequency range [50]. These become conducting upon recrystallization of the amorphous material. Resistivity changes of nearly three orders of magnitude are possible in small structures, by methods involving laser and Joule heating [51].

Table 2. Potential technologies with tunable dielectric, magnetic, and strain response for frequency-agile devices.

Method	Tunability (%)	Q	Stimulus	Frequency
Dielectric Thin Film [42]	30	45	Electric Field $E = 70$ kV/cm	1-20 GHz
Dielectric Bulk Ceramic [43]	16	>100	Electric Field $E = 15$ kV/cm	1-10 GHz
Magnetic Film [44]	15	$5 < Q < 11$	Magnetic Field 80 kA/m (1000 Oe)	0.3-5 GHz
Magnetic Bulk Ceramic [45]	3.4* (12)	<1700	Magnetic Field	7 GHz
Displacement Microstrip [46]	25* (625)	$40 < Q < 100$	Dielectric Translation (100 μm)	3-7 GHz
MEMS variable capacitor [47]	80	$100 < Q < 300$	Mechanical Displacement 1 μm	0.5-4 GHz
Varactor [48]	60	$30 < Q < 60$	Bias Voltage (20 V)	10 GHz

*Tunable frequency is proportional to the square root of the tunable permeability or permittivity, and the squares of the values are shown for comparison with the other methods (shown in parenthesis).

Silicon is a viable candidate for optically controlling conductivity. In [52], the authors reported on creating planar antennas on a silicon wafer by precisely forming plasma channels in the shape of the desired antenna. Varying the conductivity of silicon using an IR LED was reported for a reconfigurable patch antenna [53], and for a partially adaptive array with broadband monopoles [54].

6.2 Tunable Permittivity

A number of approaches have been explored to achieve economical solutions for a high ability to tune with low losses and fast response, for the purpose of controlling microwave filters and phased arrays. The relative "tunability" of the permittivity of a system is defined as

$$n_r = \frac{\varepsilon_r(0) - \varepsilon_r(E)}{\varepsilon_r(0)}, \tag{2}$$

where $\varepsilon_r(0)$ and $\varepsilon_r(E)$ are the small-signal relative permittivities without bias and with a bias of strength E [V/cm], respectively. Tunabilities as high as 75% have been reported for $(\mathrm{Ba,Sr})\mathrm{TiO}_3$ thin films at 1500 kV/cm [55]. A high electric field is required to generate a large tunability; however, the tuning voltage is low (< 25 V) because the films are in the nanometer-thickness range. A figure-of-merit for tunable dielectric devices has been established, which includes the device loss [56]:

$$K = \frac{Q(0)Q(V_{max})(n_r - 1)^2}{n_r}, \tag{3}$$

where Q is the inverse of the device's loss; $Q(0)$ and $Q(V_{max})$ are at zero bias and at the maximum voltage, respectively; and n_r is the tunability from Equation (2). K factors as high as 500 have been reported for paraelectric SrTiO_3 thin films on SrRuO_3 conductors.

Dielectric materials with the highest tunability have paraelectric/ferroelectric transition temperatures that are below the operating temperature. The magnitude of the tunability is directly proportional to the dielectric permittivity, which approaches 1,000 for materials with the highest tunability [58]. The intrinsic dielectric loss increases with frequency, which may be a concern as the operating frequency increases into the mm-wave range [59].

The dielectric permittivities of thin films and bulk materials are altered through an externally applied electric field. Large changes in permittivity under a dc voltage bias have been demonstrated in epitaxial paraelectric $\mathrm{Ba}_{0.5}\mathrm{Sr}_{0.5}\mathrm{TiO}_3$ ("BST") thin films that are deposited on single-crystal LaAlO_3 and MgO substrates [42]. The loss of the dielectric film is represented as an average Q value between the zero-field and high-electric-field bias. Bulk BST ceramics offer high tunability, and have higher Q values that BST films. Recent results have shown that high electric fields can be applied to bulk ceramics with nanometer-sized grains, corresponding to higher high overall tunability [43].

6.3 Tunable Permeability

Similar to the tunable response in dielectric materials, the magnetic permeability decreases with the application of a static field. An early example of a 1.4 cm by 1.8 cm rectangular microstrip patch was printed on a 1.27 mm thick ferrite substrate (Trans-Tech G-113 YIG), and was fed with a coaxial probe near the edge of a long dimension [60]. The center design frequency was 4.6 GHz, which was tunable over a 40% bandwidth when it was magnetically biased in the plane of the substrate, and perpendicular to the resonant dimension. The polarization response of patch antennas on garnet single crystals has also been studied at 5 GHz for externally applied magnetic fields of 600 G. One advantage of higher permeability over high permittivity is that the effective patch dimensions can be reduced, without sacrificing bandwidth [61]. There are fundamental materials limitations for tunable magnetic materials, because the permeability and the highest operating frequency are inversely related [62]. Ferrites are a class of high-frequency magnetic materials with low eddy current and hysteretic losses [63].

Tunable magnetic structures have thin-film and bulk-ceramic forms. Conformal Permalloy films (120 nm thick) were deposited on CMOS structures, having lower conduction and hysteresis losses than bulk NiFe in the GHz frequency range [44]. In addition, eddy-current losses at high frequency were minimized through the inductor's design. Judicious patterning of the magnetic film raises the ferromagnetic resonance, and hence the operating frequency, of the tunable thin-film inductors; however, the magnetic-film technology will be limited to frequencies below 10 GHz, because of the limitation in the ferromagnetic resonance frequency. There are fundamental material limitations for tunable magnetic materials, because the magnitude of μ_r and the highest operating frequency are inversely related [62]. The magnetic response of ferrites is limited to below the K band [64]. Bulk-ceramic ferrite plugs were placed within the center of a dielectric resonator operating in the $\mathrm{TE}01\delta$ mode [45]. The resonator was placed on top of a coil, which was used to apply the dc magnetic field. A high *Q* value was reported because of the low-loss dielectric resonator within the tunable structure.

6.4 Tunable Mechanical

Tunable mechanical materials are also known as active materials, and they change shape when exposed to an electric, magnetic, or thermal stimulus. Electrostrictive materials strain under an applied electric field. Magnetostrictive materials change shape due to an applied magnetic field. A magnetic field applied to a ferromagnetic material aligns the magnetic domains, and increases the length of the material in the direction of the magnetic field.

Shape-memory materials change shape due to a temperature change. Both alloys and polymers have been shown to exhibit this change. Shape-memory materials return to their original shape or size when deformed and subjected to an appropriate stimulus. The first shape-memory alloy, Nitinol (*Ni*ckel *Ti*tanium *N*aval *O*rdance *L*aboratory), was discovered in the early 1960s [65]. Today, copper-aluminum-nickel, copper-zinc-aluminum, nickel-titanium, and iron-manganese-silicon are other commonly used examples of alloys that when plastically deformed at a relatively low temperature, return to their original shape when subjected to a high temperature. Some shape-memory alloys, like Ni-Mn-Ga, respond to magnetic fields [66]. Shape-memory polymers (SMPs) are the polymer equivalent of shape-memory alloys. Light-induced shape-memory polymers are also available [67]. Lu and Kota outlined the use of shape-memory materials to adaptively deform reflector antennas from a parabolic to a spherical shape, or to tilt the reflector's surface [68].

The strain response of active materials is summarized in Table 3. Piezoelectric, electrostrictive, and Maxwell stress-based actuations are mechanical responses to an applied electric field. Piezoelectricity is generally limited to non-centro-symmetric crystal structures, and $\mathrm{Pb(Zr,Ti)O_3}$ ("PZT") ceramics are commonly used for actuator applications. Exceptionally high piezoelectric coefficients have been discovered for $\mathrm{Pb(Mg,Nb)O_3}$-$\mathrm{PbTiO_3}$ ("PMN-PT") single crystals, which have strain values exceeding 1%. Electrostriction is possible in all materials, and the highest strains are found in PMN-PT ceramics and ferroelectric poly(vinylidene fluoride-trifluoroethylene) polymers. Maxwell stresses, created by the electrostatic attraction between oppositely charged conductor plates, cause very high strains in compliant polymers, such as silicone.

Only the strain parameters are shown in Table 2, and additional requirements must be considered for implementation of active materials into a tunable device. For example, the elastic modulus of high-strain polymers is low, and will limit the total force available to move a tunable structure. Piezoelectric materials have hysteretic strain behavior at high electric

Table 3. The strain responses of several types of active materials.

Actuation Mechanism	Piezoelectric	Electrostriction	Maxwell	Magnetostriction	Phase Change
Materials	PZT, PMN-PT single crystal	PMN-PT ceramics and PVDF	Silicone	Terfernol	Nitinol
% strain range	0.1 to 1.5	0.1 to 4	20	0.2	6
Reference	[69]	[70]	[71]	[72]	[72]

fields, which may limit reproducibility in the strain response. The time response and reversibility of the phase transition in Nitinol will limit its use for fast tuning systems.

Tunable micro-electromechanical system (MEMS) and microstrip structures take advantage of piezoelectric or electrostatic forces to move capacitor plates. Tunable microstrip configurations, based on translatable superstrates above ring resonators, offer high tunability and Q values [46]. A variable MEMS capacitor has been demonstrated. The capacitance changed from 1.2 pF to 0.25 pF as the voltage was altered from 15 V to 10 V. The Q factor was high, because the structure was fabricated from high-resistivity silicon [47].

There are several challenges in comparing tunable devices that have a range of impedance, Q, and tunability parameters. Figures-of-merit have incorporated all of these parameters and have been tailored to specific devices, such as phase shifters [40]. In addition, device-performance metrics, such as temperature stability, RF power, response time, and cost, must also be considered [48]. In Table 1, the device tunability is defined by different parameters, and depends on the physical mechanism. For example, the MEMS, dielectric devices, and varactors depend upon a permittivity or capacitance change. The magnetic devices depend upon a permeability or inductance change. The magnetic bulk-ceramic and displacement-microstrip methods that are listed in Table 3 are defined by tunable frequency: hence, these values are squared, to provide a meaningful comparison with the other methods. From Table 3, it is apparent that devices that are based on mechanical strain are promising candidates for tunable devices with high Q and high tunability. In addition, these devices are not limited in frequency, as in the case of tunable magnetic materials.

7. Conclusions

Reconfigurable antennas have been around since the 1930s. Initially, they were based on mechanical movement of a feed or other antenna part. Antenna arrays took reconfigurability to a new level with the electronic control of the antenna's pattern. Semiconductor and MEMS switches have been at the heart of most reconfigurable-antenna research since the late 1990s. More recently, materials research has introduced new approaches to reconfigurable antennas, via tunable constitutive parameters and even active materials that move in response to an electrical stimulus. The need for a single antenna to perform multiple missions will continue the drive for antennas that can reconfigure themselves based upon the current need.

8. References

1. H. T. Friis, C. B. Feldman, and W. M. Sharpless, "The Determination of the Direction of Arrival of Short Radio Waves," *Proceedings of the Institute of Radio Engineers*, **22**, 1, January 1934, pp. 47-78.

2. E. Bruce and A. C. Beck, "Experiments with Directivity Steering for Fading Reduction," *Proceedings of the Institute of Radio Engineers*, **23**, 4, April 1935, pp. 357-371.

3. H. T. Friis, and C. B. Feldman, "Multiple Unit Steerable Antenna for Short-Wave Reception," *Proceedings of the Institute of Radio Engineers*, **25**7, July 1937, pp. 841-917.

4. H. T. Friis and W. D. Lewis, "Radar Antennas," *The Bell System Technical Journal*, **XXVI**, 2, April 1947, pp. 219-317.

5. R. L Haupt, *Antenna Arrays: A Computational Approach*, New York, Wiley, 2010.

6. E. W. Matthews, C. L. Cuccia, and M. D. Rubin, "Technology Considerations for the Use of Multiple Beam Antenna Systems in Communications Satellites," *IEEE Transactions on Microwave Theory and Techniques*, **27**, December 1979, pp. 998-1004.

7. A. D. Monk and P. J. B. Clarricoats, "Adaptive Null Formation with a Reconfigurable Reflector Antenna," *Proceedings of the Institute of Electrical Engineers Microwave Antennas and Propagation*, **142**, 3, June 1995, pp. 220-224.

8. J. T. Bernhard, *Reconfigurable Antennas*, San Rafael, CA, Morgan & Claypool Publishers, 2007.

9. D. A. Bathker, W. Veruttipong, T. Y. Otoshi, and P. W. Cramer, Jr., "Beam-Waveguide Antenna Performance Predictions with Comparisons to Experimental Results," *IEEE Transactions on Microwave Theory and Techniques*, **40**, 6, June 1992, pp. 1274-1285.

10. D. Jacavanco, *Reflector Antenna Having Sidelobe Suppression Elements*, US Patent 4,631,547, December 23, 1986.

11. R. L. Haupt, "Adaptive Nulling with a Reflector Antenna Using Movable Scattering Elements," *IEEE Transactions on Antennas and Propagation*, **53**, 2, February 2005, pp. 887-890.

12. A. D. Monk and P. J. B. Clarricoats, "Adaptive Null Formation with a Reconfigurable Reflector Antenna," *Proceedings of the Institute of Electrical Engineers Microwave Antennas and Propagation*, **142**, 3, June 1995, pp. 220–224.

13. B. Tomasic, J. Turtle, L. Shiang et al., "The Geodesic Dome Phased Array Antenna for Satellite Control and Communication – Subarray Design, Development and Demonstration," IEEE International Symposium on Phased Array Systems and Technology, 2003, pp. 411-416.

14. P. Rocca and R. L. Haupt, "Dynamic Array Thinning for Adaptive Interference Cancellation," Fourth European Conference on Antennas and Propagation (EuCAP), 2010, pp. 1-3.

15. W. Kummer, A. Villeneuve, T. Fong, and F. Terrio, "Ultra-Low Sidelobes from Time-Modulated Arrays," *IEEE Transactions on Antennas and Propagation*, **AP-11**, 6, November 1963, pp. 633-639.

16. "About ALMA Technology," http:// www.almaobservatory.org/, May 27, 2009.

17. National Radio Astronomy Observatory, "An Overview of the Very Large Array," http://www.vla.nrao.edu/genpub/overview/, June 17, 2009.

18. H. Steyskal, J. K. Schindler, P. Franchi et al., "Pattern Synthesis for TechSat21 – A Distributed Space-Based Radar System," *IEEE Antennas and Propagation Magazine*, **45**, 4, August 2003, pp. 19-25.

19. "Chapter 1: Understanding Key RF Switch Specifications," in National Instruments, *The Guide to Selecting an RF Switch*, http://zone.ni.com/devzone/cda/tut/p/ id/5776.

20. C. L. Goldsmith, Z. Yao, S. Eshelman, and D. Denniston, "Performance of Low-Loss RF MEMS Capacitive Switches," *IEEE Microwave and Guided Wave Letters*, **8**, 8, August 1998, pp. 269-271

21. "Solid State Switches," in the *Microwave Encyclopedia*, http://www.microwaves101.com/encyclopedia/switches_solidstate.cfm, November 18, 2010.

22. J. S. Herd, M. Davidovitz, and H. Steyskal, *Reconfigurable Microstrip Antenna Array Geometry which Utilizes Micro-Electro-Mechanical System (MEMS) Switches*, US Patent 6,198,438, March 6, 2001.

23. F. Yang and Y. Rahmat-Samii, "A Reconfigurable Patch Antenna Using Switchable Slots for Circular Polarization Diversity," *IEEE Microwave and Wireless Components Letters*, **12**, 3, March 2002, pp. 96-98.

24. L. N. Pringle, et al., "A Reconfigurable Aperture Antenna Based on Switched Links Between Electrically Small Metallic Patches," *IEEE Transactions on Antennas and Propagation*, **AP-52**, 6, June 2004, pp. 1434- 1445.

25. "The PIN Diode Circuit Designers' Handbook," Microsemi Corp., Watertown, MA, 1998.

26. D. Gotch, "A Review of Technological Advances in Solid-State Switches," *Microwave Journal*, **50**, 11, November 2007, pp. 24-34.

27. R. H. Caverly and G. Hiller, "Distortion Properties of MESFET and PIN Diode Microwave Switches," IEEE Microwave Symposium, **2**, June, 1992, pp. 533-536.

28. J. Choi and S. Lim, "Frequency Reconfigurable Metamaterial Resonant Antenna," 2009 Asia Pacific Microwave Conference, APMC 2009, 2009, pp. 798-801.

29. E. R. Brown, "RF-MEMS Switches for Reconfigurable Integrated Circuits," *IEEE Transactions on Microwave Theory and Techniques*, **46**, 11, November 1998, pp. 1868-1880.

30. S. J. Gross, S. Tadigadapa, T. N. Jackson, S. Trolier-McKinstry, and Q. Q. Zhang, "Lead-Zirconate-Titanate-Based Piezoelectric Micromachined Switch," *Applied Physics Letters*, **83**, 2009, pp. 174-176.

31. P. D. Grant, M. W. Denhoff, and R. R. Mansour, "A Comparison Between RF MEMS and Semiconductor Switches," ICMENS, August 25-27, 2004, pp. 515- 521.

32. S. Nikolaou, N. D. Kingsley, G. E. Ponchak, J. Papapolymerou, and M. M. Tentzeris, "UWB Elliptical Monopoles with a Reconfigurable Band Notch Using MEMS Switches Actuated Without Bias Lines," *IEEE Transactions on Antennas and Propagation*, **AP-57**, 8, August 2009, pp. 2242-2251.

33. G. Wang, T. Polley, A. Hunt, and J. Papapolymerou, "A High Performance Tunable RF MEMS Switch Using Barium Strontium Titanate (BST) Dielectrics for Reconfigurable Antennas and Phased Arrays," *IEEE Antennas and Wireless Propagation Letters*, **4**, 2005, pp. 217-220.

34. G. Wang, D. Thompson, E. M. Tentzeris, and J. Papapolymerou, "Low Cost RF MEMS Switches Using LCP Substrate," 34th European Microwave Conference, 2004, pp. 1441-1444.

35. P. Bhartia and BAHL, "Frequency Agile Microstrip Antennas," *Microwave Journal*, **25**, 10, October 1982, pp. 67-70.

36. N. Behdad and K. Sarabandi, "A Varactor-Tuned Dual-Band Slot Antenna," *IEEE Transactions on Antennas and Propagation*, **AP-54**, 2, February 2006, pp. 401- 408.

37. A. R. Weily, T. S. Bird, and Y. J. Guo, "A Reconfigurable High-Gain Partially Reflecting Surface Antenna," *IEEE Transactions on Antennas and Propagation*, **AP-56**, 11, November 2008, pp. 3382-3390.

38. H. Mirzaei and G. Eleftheriades, "A Compact Frequency-Reconfigurable Metamaterial-Inspired Antenna," *IEEE Antennas and Wireless Propagation Letters*, 2011, pp. 1154-1157.

39. L. Zhang, F. Yang, and A. Elsherbeni, "Analysis and Design of a Reconfigurable Dual-Strip Scanning Antenna," IEEE International Symposium on Antennas and Propagation, June 2009.

40. A. K. Tagantsev, V. O. Sherman, K. F. Astafiev, J. Venkatesh, and N. Setter, "Ferroelectric Materials for Microwave Tunable Applications," *Journal of Electroceramics*, **11**, 2003, pp. 5-66.

41. S. K. Koul and B. Bhat, *Microwave and Millimeter Wave Phase Shifters, Volume I*, Norwood, MA, Artech House, 1991.

42. J. S. Horwitz, W. Chang, W. Kim, S. B. Qadri, J. M. Pond, S. W. Kirchoefer, and D. B. Chrisey, "The Effect of Stress on

the Microwave Dielectric Properties of $Ba_{0.5}Sr_{0.5}TiO_3$ Thin Films," *Journal of Electroceramics*, **4**, 2-3, pp. 357-363.

43. S. Kwon, W. Hackenberger, E. Alberta, E. Furman, and M. Lanagan, "Nonlinear Dielectric Ceramics and their Applications to Capacitors and Tunable Dielectrics," *IEEE Electrical Insulation Magazine*, 2011 (accepted).

44. J. Salvia, J. A. Bain, and P. Yue, "Tunable On-Chip Inductors Up to 5 GHz Using Patterned Permalloy Laminations," IEEE Electron Devices Meeting, IEDM 2005, pp. 943-946.

45. J. Krupka, A. Abramowicz, and K. Derzakowski, "Tunable Dielectric Resonator Bandpass Filter," 13th International Conference on Microwaves, Radar and Wireless Communications, MIKON-2000, pp. 517-520.

46. E. Furman, M. Lanagan, I. Golubeva and Y. Poplavko, "Piezo-Controlled Microwave Frequency Agile Dielectric Devices," IEEE Frequency Control Symposium, 2004, pp. 266-271.

47. T. G. Rijks, P. G. Steeneken, J. T. M. Beek, M. J. E. Ulenaers, A. Jourdain, H. A. C. Tilmans, J. D. Coster, and R. Puers, "Microelectromechanical Tunable Capacitors for Reconfigurable RF Architectures," *Journal of Micromechanics and Microengineering*, **16**, 2006, p. 601.

48. R. Jakoby, P. Scheele, S. Muller, and C. Weil, "Nonlinear Dielectrics for Tunable Microwave Components," IEEE International Conference on Microwaves, Radar and Wireless Communications, MIKON-2004, 2004, pp. 369-378.

49. R. V. Wright, B. Chambers, A. Barnes, K. Lees, and A. Despotakis, "Progress in Smart Microwave Materials and Structures," *Smart Materials and Structures*, **9**, 2000, pp. 273-270.

50. M. Mirsaneh, E. Furman, J. V. Ryan, M. T. Lanagan, and C. G. Pantano, "Frequency Dependent Electrical Measurements of Amorphous GeSbSe Chalcogenide Thin Films," *Applied Physics Letters*, **96**, 2010, p. 112907.

51. A. L. Lacaita, A. Redaelli, D. Ielmini, F. Pellizzer, A. Pirovano, A. Benvenuti, and R. Bez, "Electrothermal and Phase-Change Dynamics in Chalcogenide-Based Memories," IEEE International Electron Devices Meeting, IEDM 2004, pp. 911-914.

52. A. E. Fathy, "Silicon-Based Reconfigurable Antennas – Concepts, Analysis, Implementation, and Feasibility," *IEEE Transactions on Microwave Theory and Techniques*, **51**, 6, June 2003, pp. 1650-1661.

53. R. L. Haupt, "Reconfigurable Patch with Switchable Conductive Edges," *Microwave and Optical Technology Letters*, **51**, July 2009, pp. 1757-1760.

54. R. L. Haupt, J. R. Flemish, and D. W. Aten, "Adaptive Nulling Using Photoconductive Attenuators," *IEEE Transactions on Antennas and Propagation*, **AP-59**, 3, March 2011, pp. 869-876.

55. C. Basceri, S. K. Streiffer, A. I. Kingon, and R. Waser, "The Dielectric Response as a Function of Temperature and Film Thickness of Fiber-Textured (Ba, Sr) TiO Thin Films Grown by Chemical Vapor Deposition," *Journal of Applied Physics*, **82**, 1997, p. 2497.

56. O. G. Vendik, E. K. Hollmann, A. B. Kozyrev, and A. M. Prudan, "Ferroelectric Tuning of Planar and Bulk Microwave Devices," *Journal of Superconductivity*, **12**, 1999, pp. 325-338.

57. H. C. Li, W. Si, A. D. West, and X. X. Xi, "Near Single Crystal-Level Dielectric Loss and Nonlinearity in Pulsed Laser Deposited SrTiO Thin Films," *Applied Physics Letters*, **73**, 1998, p. 190.

58. A. K. Tagantsev, V. O. Sherman, K. F. Astafiev, J. Venkatesh, and N. Setter, "Ferroelectric Materials for Microwave Tunable Applications," *Journal of Electroceramics*, **11**, 2003, pp. 5-66.

59. B. D. Silverman, "Microwave Absorption in Cubic Strontium Titanate," *Physical Review*, **125**, 1962, pp. 1921-1930.

60. D. M. Pozar and V. Sanchez, "Magnetic Tuning of a Microstrip Antenna on a Ferrite Substrate," *Electronics Letters*, **24**, 12, June 9, 1988, pp. 729-731.

61. R. C. Hansen and M. Burke, "Antennas with Magneto-Dielectrics," *Microwave and Optical Technology Letters*, **26**, 2000, pp. 75-78.

62. J. L. Snoek, "Dispersion and Absorption in Magnetic Ferrites at Frequencies Above One Mc/s," *Physica*, **14**, 1948, pp. 207-217.

63. J. Smit and H. P. J. WIJN, Ferrites, Phillips Technical Library, Tokyo Electrical Engineering College Press, 1965, p. 269.

64. J. Smit and H. P. J. WIJN, *Ferrites*, Phillips Technical Library, Tokyo Electrical Engineering College Press, 1965, p. 269.

65. P. K. Kumar and D. C. Lagoudas, "Introduction to Shape Memory Alloys," in D. C. Lagoudas (ed.), *Shape Memory Alloys*, New York, Springer Science, 2008, pp. 1-51.

66. K. Ullakko, "Magnetically Controlled Shape Memory Alloys: A New Class of Actuator Materials," *J. Materials Engineering and Performance*, **5**, June 1996, pp. 405-409.

67. M. Behl, J. Zotzmann, and A. Lendlein, "Shape-Memory Polymers and Shape-Changing Polymers," in A. Lendlein (ed.),

Shape-Memory Polymers, New York, Springer-Verlag, 2009, pp. 1-40.

68. K. Lu and S. Kota, "Design of Compliant Mechanisms for Morphing Structural Shapes," *Journal of Intelligent Material Systems and Structures*, **14**, June 2003, pp. 379-391.

69. S. E. Park and T. R. Shrout, "Ultrahigh Strain and Piezoelectric Behavior in Relaxor Based Ferroelectric Single Crystals," *Journal of Applied Physics*, **82**, 1997, p. 1804.

70. Q. M. Zhang, V. Bharti, and X. Zhao, "Giant Electrostriction and Relaxor Ferroelectric Behavior in Electron-Irradiated Poly (Vinylidene Fluoride-Trifluoroethylene) Copolymer," *Science*, **280**, 1998, p. 2101.

71. T. Mirfakhrai, J. D. W. Madden, and R. H. Baughman, "Polymer Artificial Muscles," *Strain*, **10**, 4, 2007, pp. 30-38.

72. I. Chopra, "Review of State of Art of Smart Structures and Integrated Systems," *AIAA Journal*, **40**, 11, 2002, pp. 2145-2187.

Introducing the Feature Article Authors

Randy L. Haupt received the BSEE from the USAF Academy (1978), the MS in Engineering Management from Western New England College (1982), the MSEE from Northeastern University (1983), and the PhD in Electrical Engineering from the University of Michigan (1987). He is a Professor and Department Head for the Electrical Engineering and Computer Science Department of the Colorado School of Mines, Golden, Colorado. He was an RF Staff Consultant at Ball Aerospace & Technologies, Corp. He was Senior Scientist and Department Head at the Applied Research Laboratory of Penn State, Professor and Department Head of ECE at Utah State, Professor and Chair of EE at the University of Nevada Reno, and Professor of EE at the USAF Academy. He was a project engineer for the OTH-B radar, and a research antenna engineer for Rome Air Development Center early in his career. He is coauthor of the books *Practical Genetic Algorithms, Second Edition* (Wiley, 2004); *Genetic Algorithms in Electromagnetics* (Wiley, 2007), and *Introduction to Adaptive Antennas* (SciTech, 2010), as well as author of *Antenna Arrays: A Computation Approach* (Wiley, 2010). Dr. Haupt was the Federal Engineer of the Year in 1993. He is a Fellow of the IEEE and of the Applied Computational Electromagnetics Society (ACES). He serves as Associate Editor for the "Ethically Speaking" column in the *IEEE Antennas and Propagation Magazine*.

Michael Lanagan received his BS in Ceramic Engineering from the University of Illinois in 1982, and his PhD from Penn State in 1987. He is presently Professor of Engineering Science and Mechanics. Before joining Penn State, Dr. Lanagan was at Argonne National Laboratory for twelve years. Prof. Lanagan's research interests are in two general areas. The first is the exploration of new materials and structures for energy-storage applications. The second research topic involves advanced materials and devices for enhanced magnetic-resonance imaging. He is an author of over 250 technical publications and 10 patents. His present interests also include synthesis, processing, and characterization of new materials for wireless communications and power electronics applications.